Appendix C

Single Counter Monte Carlo

A single lead-glass block–PMT counter Monte Carlo simulation has been developed. Some of the Monte Carlo simulation results have been described in section 4. In this appendix, a description, characteristics and results of the Monte Carlo are presented. Also included are some comparisons of the Monte Carlo results and some of the test beam studies (section 4.2).

The charged particles in the electromagnetic shower which have sufficient energy produce Čerenkov photons. The photons propagate to the PMT where photoelectrons can result. Total internal reflection is the main reason photons do not escape the block. A white paper wrapping is used to reflect photons which do not satisfy the critical angle requirement for total internal reflection. The Monte Carlo simulation tries to simulate these and other processes. The transmittance measurements through a 10 cm block of F2 lead-glass in 10 nm wavelength bands are used and are given in table C.1. The quantum efficiency as a function of wavelength for the PMTs, estimated from a data sheet provided by Hamamatsu, is also included in table C.1.

Wavelength Band (nm)		Transmittance 10 cm F2 (percent)	Quantum Efficiency (percent)
295	304	12.5	5.0
305	314	23.6	12.0
315	324	34.7	18.0
325	334	45.8	22.5
335	344	56.9	25.0
345	354	68.0	27.5
355	364	79.1	28.0
365	374	88.3	28.5
375	384	92.2	29.0
385	394	95.5	29.0
395	404	96.8	28.8
405	414	97.3	28.3
415	424	97.6	27.5
425	434	97.8	26.5
435	444	97.9	25.0
445	454	98.0	24.0
455	464	98.1	22.5
465	474	98.2	21.0
475	484	98.3	19.5
485	494	98.4	18.0
495	504	98.5	17.0
505	514	98.6	15.5
515	524	98.7	13.5
525	534	98.8	12.0
535	544	98.9	10.0
545	554	99.0	8.5
555	564	99.1	7.0
565	574	99.2	5.5
575	584	99.3	3.5
585	594	99.4	2.5
595	604	99.5	1.5

Table C.1: Transmittances and quantum efficiencies in 10 nm wavelength bands as used in the single counter Monte Carlo simulation.

C.1 Simulation

There are three parts to the Monte Carlo simulation. Since the E760 central calorimeter is designed to measure the energy of electromagnetic shower inducing particles, one part of the Monte Carlo is for the shower development. Non-showering particles require a separate simulation. Both of the above simulations pass positions and momenta of charged particles to the third part of the Monte Carlo where Čerenkov light generation and propagation of photons are simulated.

C.1.1 Electromagnetic Showers

Simulation of electromagnetic showers is done with the EGS4 code system. The radiation transport of e^+'s, e^-'s, or γ's is simulated within the proper geometries of F2 lead-glass. The EGS4 simulation includes physics processes such as Bremsstrahlung, Moliére and Compton scattering, and pair production and annihilation. All shower particles are tracked until either a particle has a position outside of the block geometry or has an energy less than 650 KeV, the Čerenkov threshold for electrons in F2 lead-glass.

Shower information about paths and energy loss per step (< 1 mm) of the particle and its secondaries is used by the Čerenkov photon generating and propagating simulation code, discussed in section C.1.3. The shower inducing particles (e^+, e^-, or γ) are assumed incident normal to the front face at a randomly chosen position in a centered 1×1 cm^2 area. The incident energy is an input variable into the Monte Carlo.

C.1.2 Non-showering Particles

Traversing particles which do not induce electromagnetic showers are simulated: charged pions, protons and cosmic ray muons. The traversal of non-showering particles is simulated by small steps (< 1 mm) with multiple small angle scattering as well as energy loss, dE/dx. Strong nuclear reactions are not simulated. After each step, the Čerenkov photon generating and propagating code is called, section C.1.3.

A check for δ ray production (knock-on electrons) from the traversal of a non-showering particle is done each step. If a δ ray has been produced, the δ ray's energy is generated from a distribution quadratic in the reciprocal of the kinetic energy of the resulting δ ray [86]. The minimum allowed Monte Carlo energy of a δ ray is 1 MeV, while the maximum is determined by the mass and energy of the non-showering particle. The direction of the δ ray is parallel to the direction of the traversing particle. The resulting position and momentum inside the lead-glass block of the δ ray is then submitted to the EGS4 code system (section C.1.1) for transport and shower development.

Pions and protons are taken to have normal incidence upon the same area as described in the previous section. The incident energy for the pions and protons is an input variable. The cosmic ray muons are simulated to have the average energy of cosmic ray muons at sea level, 2 GeV. The initial position and direction of a muon are set as two random variables which correspond with calibration tests performed at Fermilab using two scintillator paddles in coincidence above and below an upright counter (discussed in section 4.1.2). Therefore, the incident position and direction are taken random within the confining paddle geometry. For the smaller cross-sectional lead-glass blocks, it is possible for the muon, as in the cosmic ray tests, to enter the blocks through a side face missing the front face, thus having a shorter traversing path length through the block.

C.1.3 Čerenkov Photons

After a charged particle is stepped, the average β for the step is used to generate Čerenkov photons; the position and momentum of the charged particle is passed from the other parts of code discussed in sections C.1.1 and C.1.2. The Čerenkov photons are generated in 10 nm wavelength bands (the bands in table C.1). The first set of Monte Carlo simulations only generated Čerenkov light between 350 nm and 600 nm. The Monte Carlo was extended to include wavelengths down to 300 nm. The photons are propagated to one of three fates: the photons can be absorbed, escape the block, or hit the PMT face.

After a photon at a certain wavelength has been generated, a random number generator is used to calculate the absorption distance using the appropriate value of transmittance from table C.1 At every surface that a photon hits, the total distance travelled by the photon is calculated. If the photon's travel distance is greater than the photon's absorption distance, the photon is considered to have been absorbed by the lead-glass.

The reflection part of the Monte Carlo has undergone some changes. Originally, only total internal reflection was used to propagate photons which hit any face. The simulation has been changed to calculate a Fresnel coefficient for a photon that does not undergo total internal reflection. Since the Fresnel coefficients depend upon the photon polarization with respect to the plane of incidence, the polarization of the incident photon is taken in accord with the Čerenkov effect: polarization is in the plane of the charged particle and photon momenta. To choose which Fresnel coefficient to calculate (parallel or perpendicular to plane of incidence), the dot product of the polarization vector and the plane of incidence is used. A random number generator is used to determine which Fresnel coefficient to calculate and then whether the photon is reflected. The Monte Carlo has been further developed by incorporating reflection from the white paper wrapped around each counter. Since paper is not a specular reflector, a cosine distribution is used for the reflected direction of the photon and the polarization is random. Another Fresnel coefficient is calculated and used to see if the photon is reflected off the the outside of the block. If reflected, the photon is considered to have escaped; otherwise, the photon is refracted and further propagated in the block. The paper is only simulated on five of the sides (not the back face).

When a photon does not get absorbed or lost, and reaches the back face, a check is made to see if the photon hits the PMT face (a circular area of the correct size centered on the block's back face, table 3.1). If the PMT face has been hit, then the quantum efficiency for the wavelength band is used to determine whether or not a photoelectron results. If the photon does not hit the PMT face, the photon is subjected to the same treatment as described above for reflection except there is no paper. However, there exists a set of Monte Carlo simulations which includes paper reflections for the back face. There is also a set of simulations where the blocks are wrapped in aluminum foil, which has a 90% chance of specular reflection for non-internally reflected photons. The final Monte Carlo has paper on the five sides allowing for paper reflections for escaped photons.

C.2 Characteristics and Effects

Several characteristics of the Monte Carlo have been studied. All aspects of the Monte Carlo were kept in a large bookkeeping operation, split into the three areas of simulation. Below are the characteristics of each area of simulation along with the effect of different simulated physics processes on the final photoelectron results.

C.2.1 Electromagnetic Showers

A fictitious large block geometry (30 cm $\times$ 30 cm $\times$ length of a block) was used to see how an electromagnetic shower develops. In figure C.1, the radial distance from the incident axis for all generated Čerenkov photons is shown. The number of Čerenkov photons generated along a charge particle's path is dependent upon

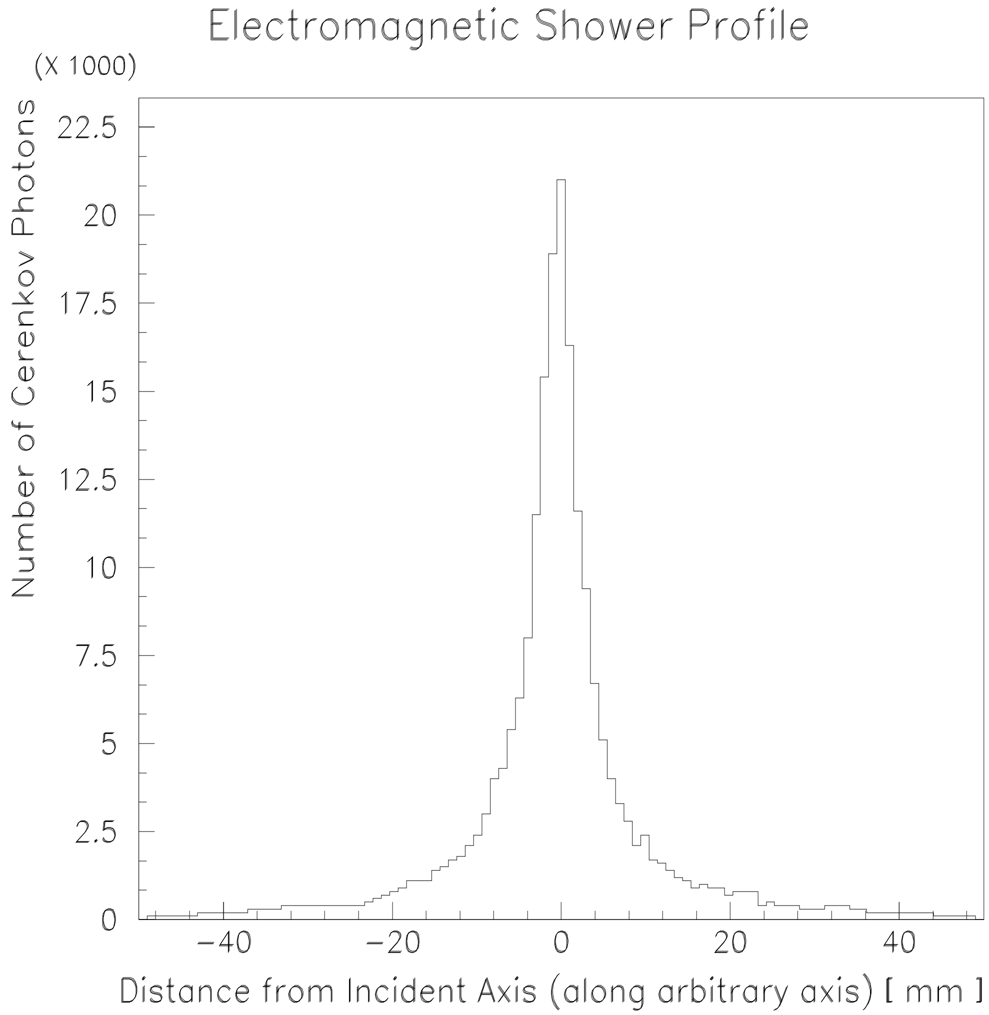

Figure C.1: The electromagnetic shower width as the number of Čerenkov photons generated as a function of distance from the incident axis along an arbitrary axis for 3 GeV incident electrons.

β. As the shower develops, the particles become less energetic, thus β becomes smaller and the particles are less efficient in producing Čerenkov light. The shower FWHM shown in figure C.1 is 7 mm which is in agreement with the Molière radius of 5 mm for F2 lead-glass. The width of the simulated shower has been determined to be independent of incident energy. The Čerenkov generation of photons along the

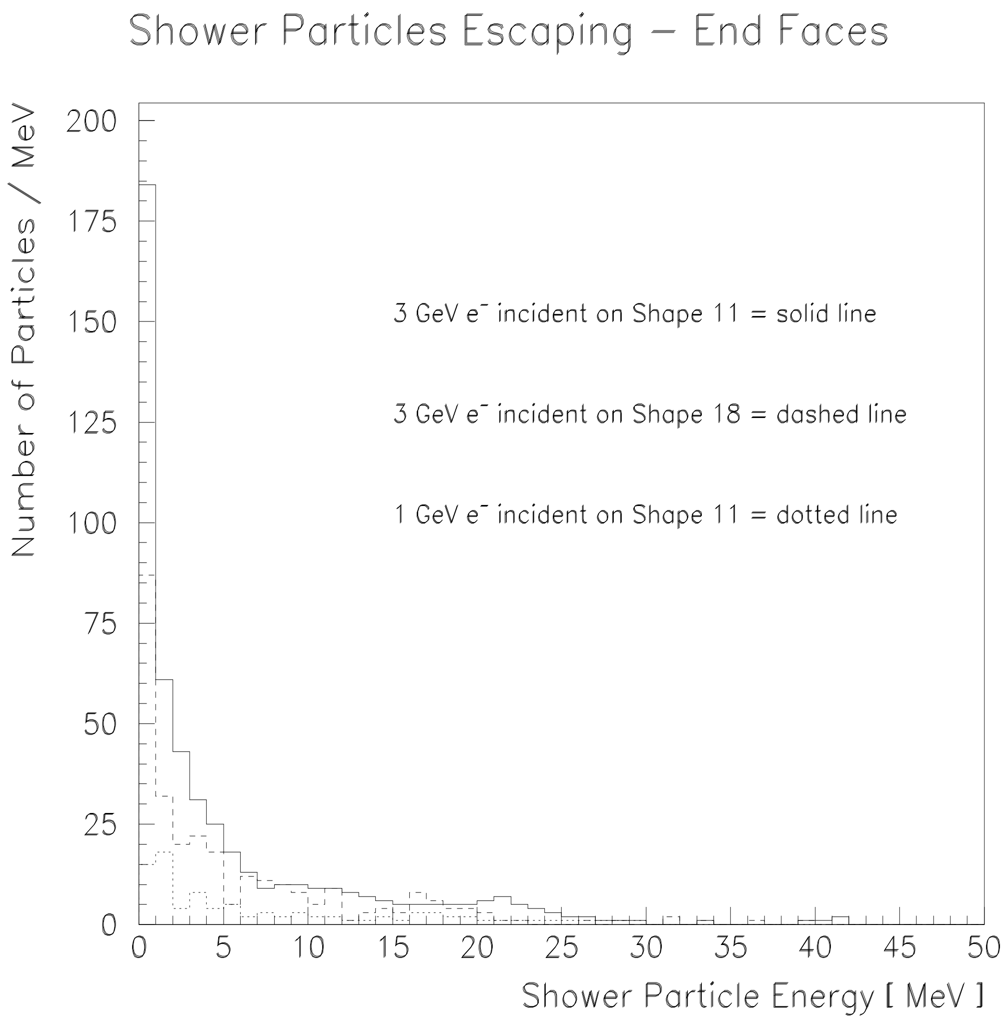

Figure C.2: The energy distribution of shower particles escaping through the end faces.

incident axis has been found to be maximum at a depth (distance from the front face) of 15.8 and 19.2 cm for 1 GeV and 3 GeV incident electrons, respectively.

For most shapes the centered electromagnetic shower is generally contained within the block. The number of Čerenkov photons generated within each shape is compared with the number generated in the large fictitious block. The larger blocks contain approximately 90% of the possible Čerenkov photons. As the cross-sectional

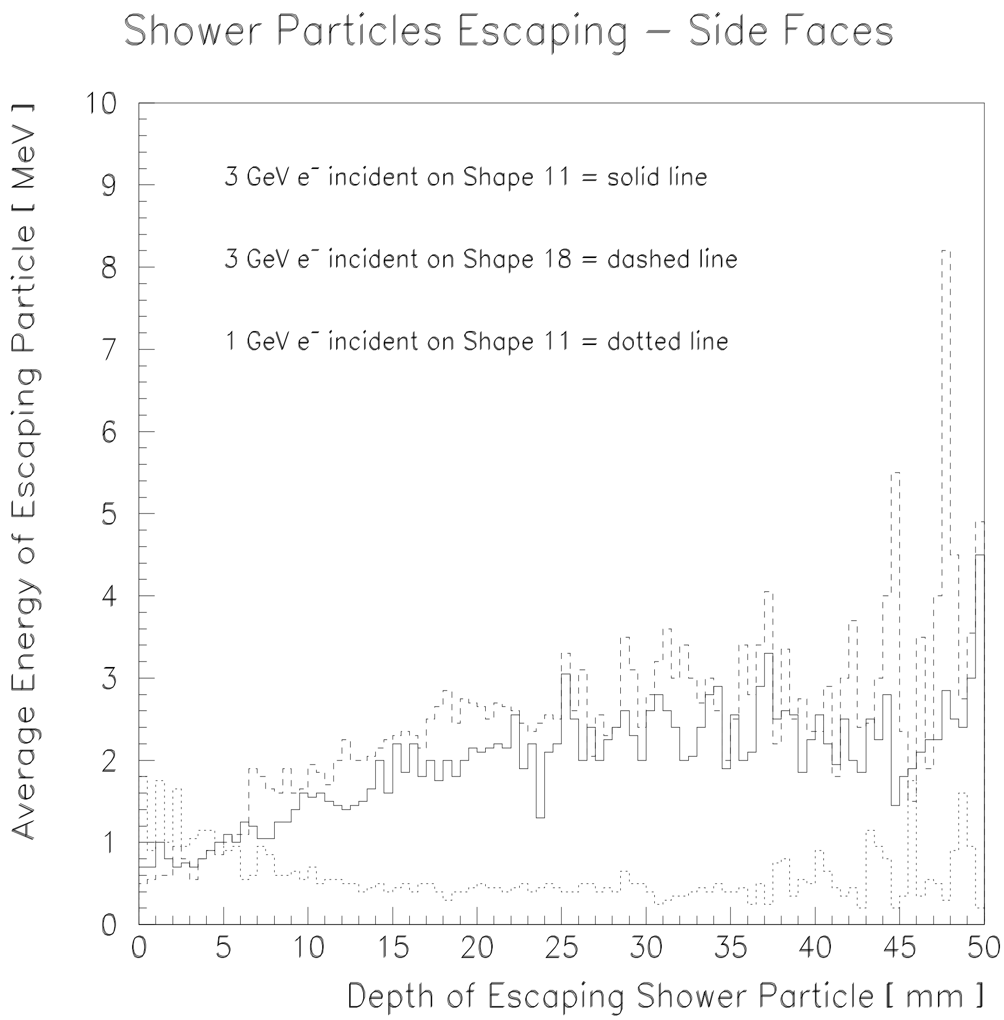

Figure C.3: The average energy of escaping shower particles through the side faces as a function of depth into a counter.

area of the blocks decreases, the percentage contained within the block decreases (see tables C.8 and C.9).

The electromagnetic shower particles which leave the blocks were investigated. Most of the particles escaping the blocks have energies less than 10 MeV. Particles escaping the end faces of shape 11 have average energies of 4.5 and 4.6 MeV for 1 and 3 GeV incident electrons. For 3 GeV electrons incident upon shape 18, the

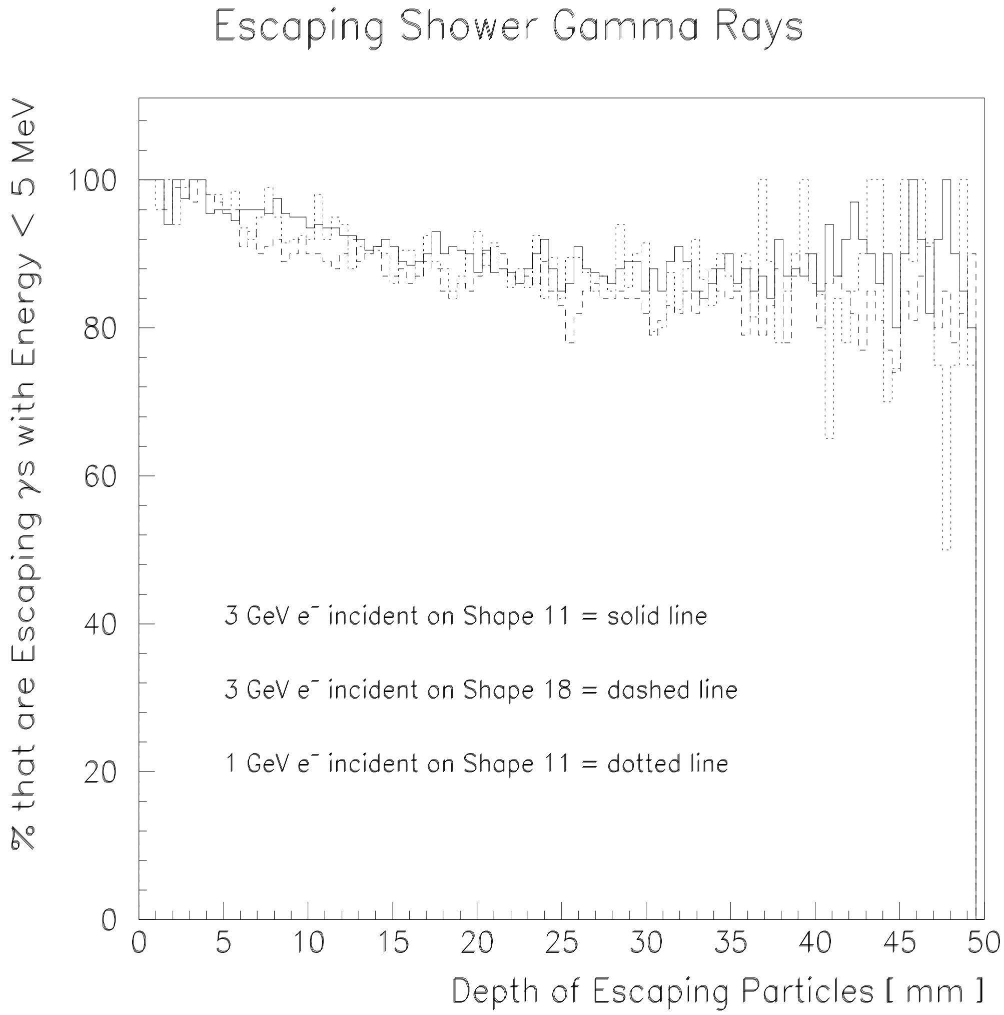

Figure C.4: The percentage of the escaping electromagnetic shower particles that are gamma rays with less than 5 MeV as a function of depth.

average shower particle escaping the end faces was found to be 6.9 MeV. Figure C.2 shows the average number of shower particles escaping the end faces for a hundred simulations of the three cases stated above. Particles leaving the side faces have smaller average energies, 1.8 and 2.0 MeV for 3 GeV incident electrons into shapes 11 and 18, respectively. For 1 GeV electrons incident upon shape 11, the average escaping particle energy decreases to 0.7 MeV. Figure C.3 shows the average shower particle energy as it leaves the block as a function of depth. Most of the escaping particles

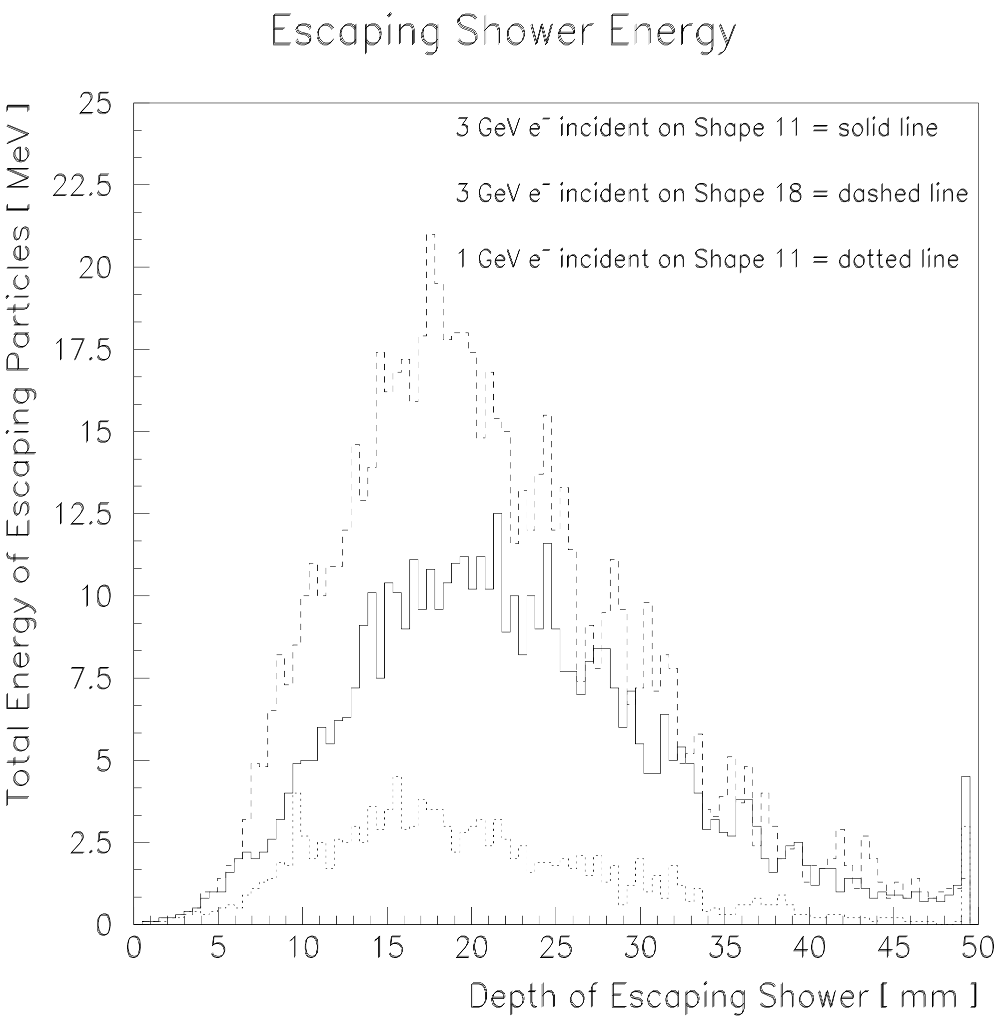

Figure C.5: The shower energy escaping through the side faces as a function of depth.

have been determined to be γ rays with energies < 5 MeV as seen in figure C.4. The total energy that leaves as a function of depth averaged over a hundred simulations is shown in figure C.5. Table C.2 shows the number of particles and the sum total of energy escaping the counters in the three simulations.

		Escaped Electromagnetic Shower			
	Incident	Side Faces		End Faces	
Block Number	Energy (GeV)	# of Particles	Energy (MeV)	# of Particles	Energy (MeV)
11	1	71.0	169.3	0.81	3.7
11	3	247.3	484.7	3.97	18.3
18	3	312.2	726.7	2.35	16.3

Table C.2: The average number of shower particles escaping and average total energy of the escaping particles for 100 Monte Carlo simulations.

C.2.2 Non-showering Particles

The average energy lost by pions and muons traversing a 50 cm block due to dE/dx has been found to be 270 MeV. For protons, 200 MeV has been determined to be the average energy lost while passing through the longest blocks. The average distance that a non-showering particle exits the back end face of a block from the exit point calculated from a straight path, caused by multiple small angle scattering, is 1.6 and 2.6 mm for incident energies of 4 and 2.5 GeV, respectively. Of 1000 incident protons or pions with incident energies of 4 and 2.5 GeV, the largest displacements from a straight path are 5 and 8 mm. The same holds true for cosmic ray muons

Particle type	Incident Energy (GeV)	Number of δ rays	Average δ ray Energy (MeV)	Maximum δ ray Energy (MeV)	Total δ ray Energy (MeV)
Pion	2.5	12.4	4.8	286.0	61.7
Proton	2.5	7.3	2.2	6.1	4.0
Pion	4.0	12.6	6.6	686.0	72.0
Proton	4.0	10.0	2.8	17.3	13.4

Table C.3: δ ray production as a function of energy and incident particle type averaged for 1000 simulations.

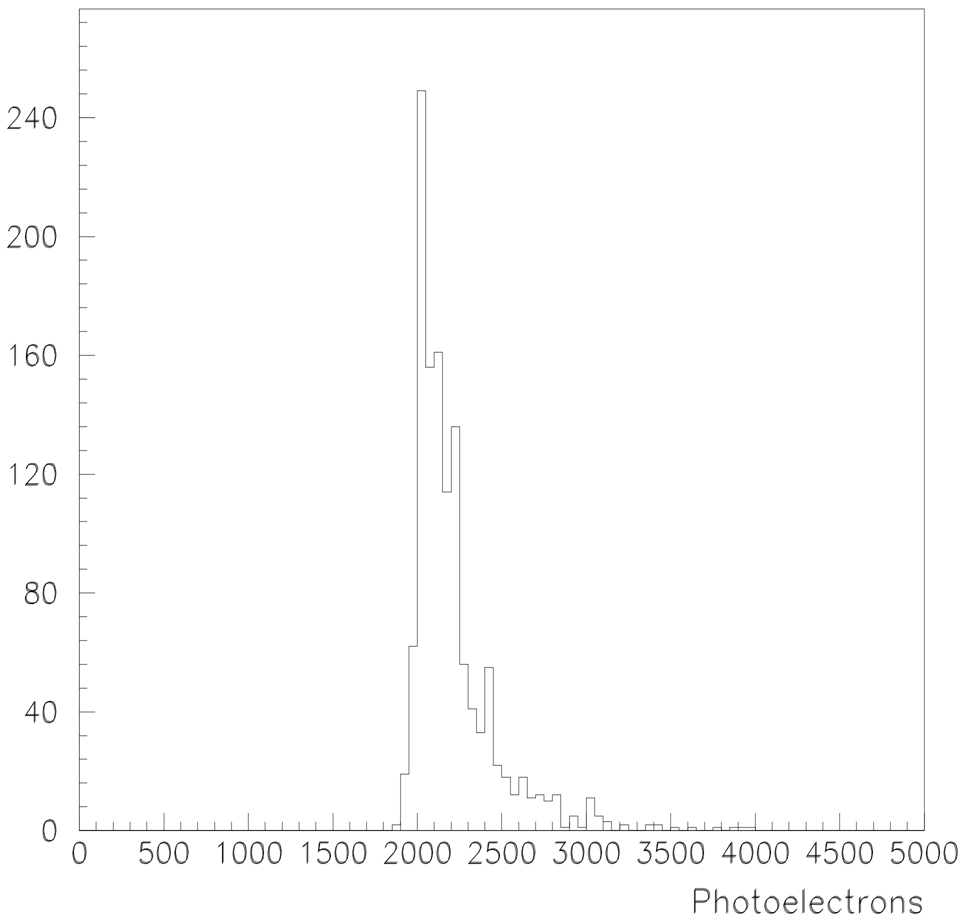

Figure C.6: The results of 1000 Monte Carlo simulations of 3 GeV incident pions into shape 11.

which intersect the front face of a block; up to 30% of cosmic ray muons do not enter through the front face of the smaller shapes.

The energy of a δ ray is a function of the incident particle's energy and mass. In table C.3, the average δ ray energy generated and the theoretical maximum energy of a δ ray are shown. Also shown is the average summed energy of all the δ rays produced from one traversing non-showering particle. The average energy of the

δ rays generated increases with increasing incident energy and decreases with heavier incident particle mass.

The total number of resulting photoelectrons is affected to some extent by the addition of the three physical processes stated above. When dE/dx is added to the simulation the photoelectron output decreases by 8%. A decrease of 2% occurs when multiple small angle scattering is included. Production of δ rays causes the resulting photoelectron spectrum to be a gaussian with a high side tail, as shown for a thousand simulations in figure C.6. The average mean number of photoelectrons increases by 8% from the δ ray production.

C.2.3 Čerenkov Photons

The simulation of the propagation of the Čerenkov photons has been developed for a period of time, allowing studies of each new simulated process. The easiest bookkeeping involved is the statistics of the fates of all Čerenkov photons generated. As an example, table C.4 shows the number of photons which suffer each fate and the resulting number of photoelectrons for shape 11. Since the photons are generated in the 10 nm wavelength bands shown in table C.1 with a $\frac{1}{\lambda^2}$ dependence, all frequency dependent processes are done within the wavelength bands.

There is at least a 40% chance that a photon will hit the PMT from any depth in the lead-glass blocks. The percentage of generated photons which hit the PMT as a function of depth at which they are generated is shown in table C.5 for shape 11.

Photon Fate	Electrons 1 GeV	Electrons 3 GeV	Cosmic Muons	Beam Pions
Generated	61650	186400	27040	26660
Absorbed	28340	84830	11450	11260
Escaped	8110	24190	1860	1450
Hit PMT	25200	77380	13730	13950
Photoelectrons	4911	15080	2724	2837

Table C.4: The fates of Čerenkov photons for a Monte Carlo event.

Depth (cm) Electrons 1 GeV	Depth (cm) Electrons 3 GeV	Depth (cm) Cosmic Muons	Depth (cm) Beam Pions	Hit PMT Percentage $\geq$
0	0	0	0	40%
33	35	14	16	45%
38	41	27	20	50%
47	46	44	42	60%
49	49	48	46	70%
$\cdots$	$\cdots$	$\cdots$	47	80%
$\cdots$	$\cdots$	$\cdots$	49	90%

Table C.5: The Percentage of Čerenkov photons which hit the PMT as a function of the depth of generation. The data is for Monte Carlo response simulation of shape 11; the PMT is at 50 cm.

Center of 10 nm band of Wavelengths (nm)	Average Distance Propagated to PMT (cm)			
	Electrons		Cosmic	Beam
	1 GeV	3 GeV	Muons	Pions
300	8.7	8.9	4.8	4.4
320	27.4	23.6	9.7	8.9
350	45.4	41.1	22.3	21.0
370	58.3	54.7	36.4	34.6
400	76.3	74.5	55.4	52.6
450	82.0	80.1	60.6	56.9
500	84.5	83.1	63.6	60.0
550	87.6	86.5	67.1	63.3
600	90.5	89.6	70.6	65.5

Table C.6: The average distance that Čerenkov photons travel that hit the PMT

Since the pions are incident along the axis of the lead-glass block, the photons of the Čerenkov cone are within the critical angle for total internal reflection; therefore, the Čerenkov photons from pions are *focused*. The photons caused by cosmic ray muons are not as focused since the muons are not constrained to be along the axis of the lead-glass block, causing part of the cone not to be internally reflected. The generated angle of the Čerenkov photons with respect to the axis of the block (the perpendicular to the front and back faces) is shown in figure C.7 in terms of the cosine of that angle; note that $\cos\theta_C = \frac{1}{n} = 0.617$ for $\beta = 1$. The backward photons of the pion simulations are caused by δ ray induced showers.

The above focusing helps to shorten the distance that the photons travel to the PMT. In table C.6, the average distance is shown for Čerenkov photons which hit the PMT. The electromagnetic shower Čerenkov light production is spread out and is closer to the front face than the PMT. If the shower extends to near the PMT, the charged particles have low energy and are directed randomly causing the Čerenkov

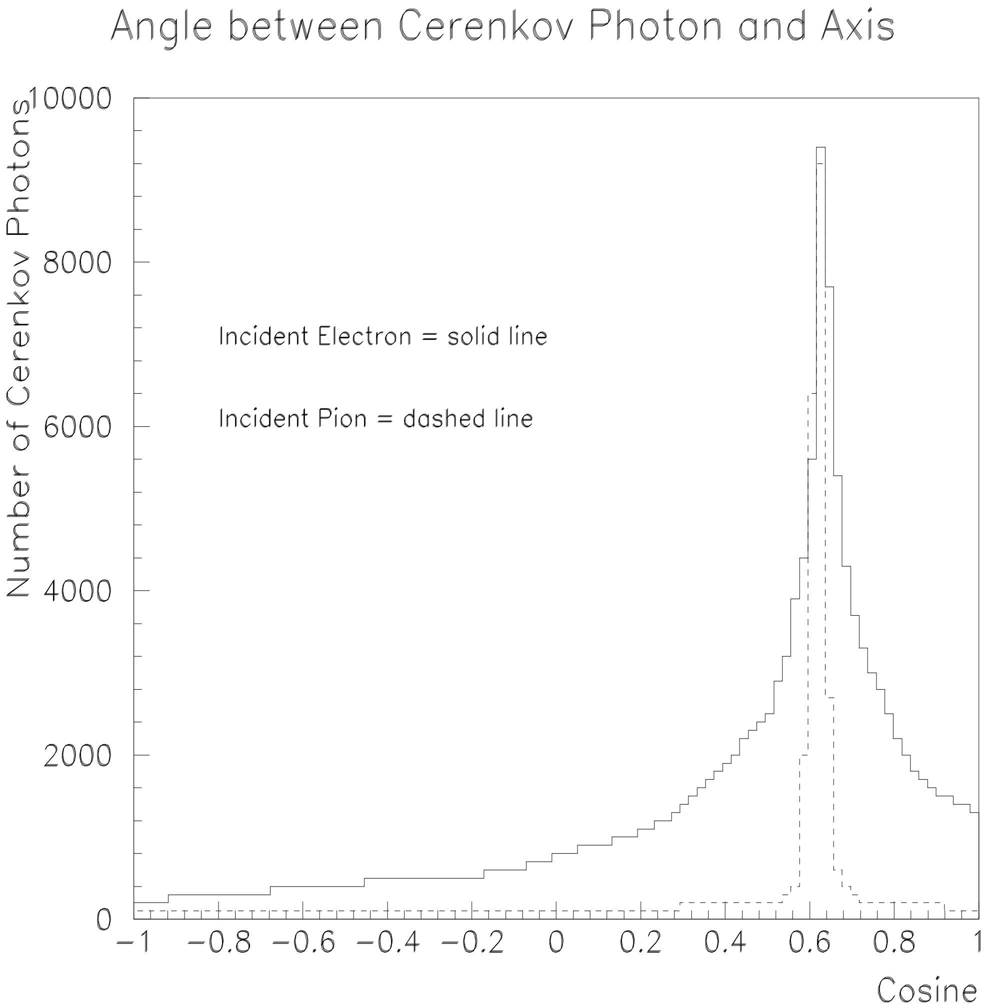

Figure C.7: The angular distribution (the angle between the Čerenkov photon momentum vector and the incident particle direction, the axis of symmetry of the lead-glass block) of Monte Carlo generated Čerenkov photons for incident electrons and pions.

Number Of Paper Reflections	Electrons 1 GeV (%)	Electrons 3 GeV (%)	Cosmic Muons (%)	Beam Pions (%)
0	70.20	69.70	87.14	89.52
1	24.70	24.50	10.03	8.33
2	4.30	4.85	2.29	1.77
3	0.66	0.79	0.44	0.32
4	0.10	0.12	0.07	0.05
5	0.02	0.02	0.01	0.01
6	small	small	small	small
7	small	small	small	small
8	none	small	small	none
9	small	small	none	none

Table C.7: The percentage of photons which hit the phototube and the number of paper reflections.

photons to be generated almost isotropically. A non-showering particles produces Čerenkov light consistently along its path.

A paper wrapping to reflect non-internally reflected photons back into the lead-glass block increases the PMT output. Table C.7 shows the percentage of the total number of photons which hit the PMT for shape 11 as a function of the number of paper reflections. As can be seen, the addition of paper affects Čerenkov photons from electromagnetic showers more than the non-showering particles. The average total number of reflections in a shape 11, internal and paper, is 12.2 for 1 and 3 GeV electrons, 8.2 for pions, and 8.8 for cosmic ray muons.

The number of photons (in the 10 nm wavelength bands) which suffer each fate has been determined. Figure C.8 shows the percentage that result in each fate for the photons created by a 3 GeV electron and a 3 GeV pion incident upon shape 11. In figure C.9, the distributions of photons generated, absorbed, hit the PMT, and which

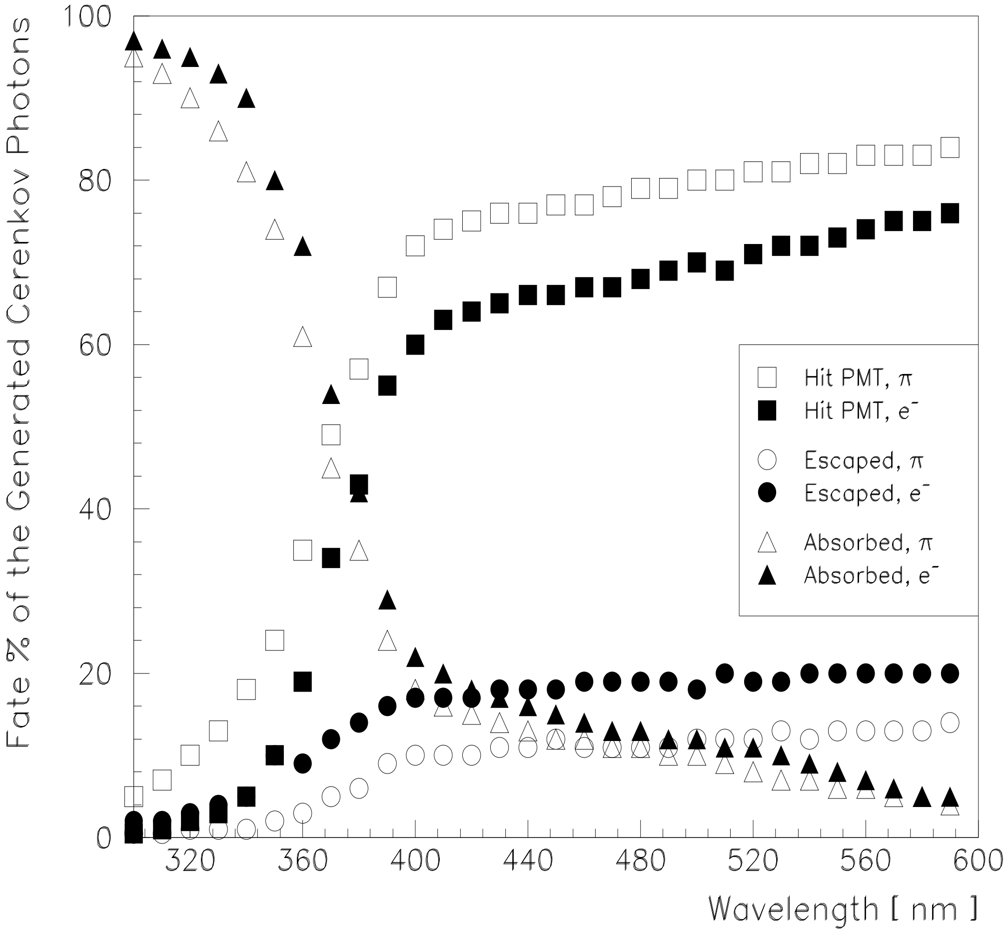

Figure C.8: The percentage of the generated Čerenkov photons which are absorbed, escape the counter, or hit the PMT.

cause photoelectrons are shown for both incident 3 GeV electrons and pions. The $\frac{1}{\lambda^2}$ Čerenkov spectrum of photons generated is apparent. The absorption of ultraviolet is shown dramatically since it is weighted by the Čerenkov spectrum for the absorbed photon distribution. The spectrum for the photons which result in the creation of photoelectrons is essentially the quantum efficiencies from table C.1 multiplied with the hit PMT photon spectrum.

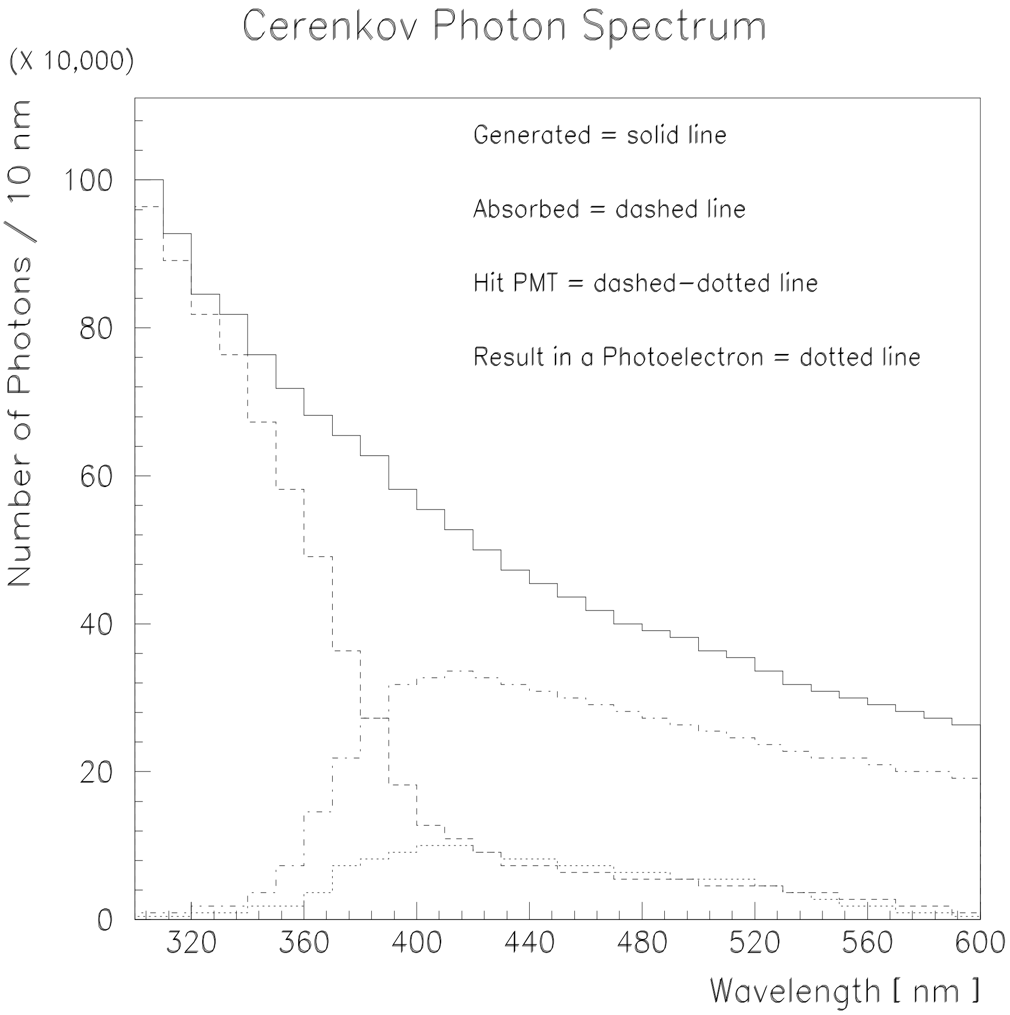

Figure C.9: The Čerenkov photon distributions for generated photons, absorbed photons, photons which hit the PMT, and photons which produce a photoelectron.

The different additions to the Monte Carlo have affected the photoelectron results differently for the shower inducing particles and the non-showering particles. The addition of the wavelengths between 300 nm and 350 nm increased the photoelectron results by 5.3% and 9.1% for 1 GeV incident electrons and cosmic ray muons, respectively, compared to Čerenkov light only being produced between 350 nm and 600 nm. The addition of ultraviolet wavelengths affected the non-showering particles more than the electromagnetic showers. Photons which were not within the critical angle and were reflected according to the probability of reflection from Fresnel equations increased the photoelectron output by 7.5% and 1.9%, a greater effect for electromagnetic showers. The addition of paper wrapping to all sides except the back face increased the incident electron result by an additional 43.5% while the cosmic ray muon result increased by 21.4%. If paper was included on the back face (all surfaces papered except where the PMT is attached), the electron and cosmic ray muon results increased 7.4% and 3.5%, respectively. When aluminum foil was simulated as the wrapping, increases of 47% and 17% were obtained for electrons and cosmic ray muons, respectively, with respect to the internally reflected results (no Fresnel reflections).

C.3 Monte Carlo Results

Below are the results of a thousand simulations of each type of event for all the shapes. The results are for Čerenkov light generated between 300 nm and 600 nm with paper on five sides; the transmittance and quantum efficiency are in table C.1. The number of photoelectrons is directly proportional to ADC channel number; the ADC channel is the gain of the PMT multiplied by the number of liberated photoelectrons. Therefore, ratios of the number of Monte Carlo photoelectrons for different cases can be compared with ratios of ADC channels for different tests.

Block Shape Number	Energy Deposited in Block (MeV)	Energy Deposited Percent of Large Glass	Generated Photons in Block	Generated Photons Percent of Large Glass	Photo-electrons in PMT
1	850	89.6	62620	93.8	4043
2	857	90.2	63270	94.6	4073
3	860	90.4	63250	94.4	4001
4	861	90.1	63380	94.3	3953
5	865	90.2	63520	94.2	3864
6	861	89.1	63540	94.0	3774
7	862	88.6	63400	93.5	3674
8	860	88.2	63420	92.3	3753
9	858	88.0	63190	91.9	3900
10	861	88.3	63430	92.3	4090
11	859	88.1	63390	92.2	4251
12	859	88.1	63360	92.2	4450
13	859	88.1	63360	92.2	4602
14	850	87.2	62710	91.2	4697
15	831	85.2	61960	90.1	4150
16	823	84.4	61460	89.4	4691
17	799	82.0	60210	87.6	3881
18	780	80.0	59050	85.9	4356
19	756	77.6	57660	83.9	3299
20	728	74.7	55820	81.2	3667

Table C.8: Monte Carlo response of a single counter to 1 GeV incident electrons.

C.3.1 Electromagnetic Shower Inducing Particles

1 GeV incident electrons have been simulated for all twenty shapes and the results are presented in table C.8. The third and fifth columns of table C.8 compare the individual shapes to the imaginary large piece of lead-glass. The energy deposited in the first fourteen shapes is about 86% of the incident electron's energy or 89% of the energy deposited in the large block. The shower width becomes larger than the width of the smaller blocks and there is a fall off to 73% of the incident energy deposited in shape 20. A larger percentage (93% for the first fourteen shapes decreasing to 81%)

of the Čerenkov photons are generated within the shapes compared to the large piece of lead-glass. The charged shower particles outside of the shapes, but inside the large piece of lead-glass, have smaller energies and do not generate as much Čerenkov light since β approaches $\beta_{threshold} = \frac{1}{n}$. The last column shows the mean number of resulting photoelectrons. The number of photoelectrons increases with block number when the percentage of area covered by the PMT increases. The decreases occur when the blocks become smaller and a smaller sized PMT is attached covering a smaller percentage of the back face (see table 3.1).

Shower fluctuations will cause a distribution of the resulting number of photoelectrons. Defining resolution as FWHM/mean, the resolution for most of the blocks is between 0.06 and 0.12 for energy deposited in a block for 1 GeV incident electrons. The resolution is dependent upon the width of the block. This dependency is also seen in the fluctuation (FWHM/mean) of the number of Čerenkov photons generated (0.07 to 0.12) and photoelectrons observed (0.10 to 0.15).

Table C.9 has the same format as table C.8 for 3 GeV incident electrons. The percent of initial energy deposited is the same as for 1 GeV incident electrons for the longer blocks. The first five blocks are a few percent smaller since showers extend past the ends of these blocks. However, when compared to the large piece of lead-glass, the same percentage results for energy deposited as 1 GeV incident electrons. The ratios of generated photons between tables C.9 and C.8 are nearly three except for the shorter shapes which have ratios slightly less than three. The percentage of the large lead-glass Čerenkov photons generated within the shape is nearly the same

Block Shape Number	Energy Deposited in Block (MeV)	Energy Deposited Percent of Large Glass	Generated Photons in Block	Generated Photons Percent of Large Glass	Photo-electrons in PMT
1	2487	90.4	183300	92.3	12410
2	2516	92.5	185300	93.2	12460
3	2523	90.4	185900	93.3	12340
4	2531	90.7	186600	93.4	12160
5	2548	90.7	187700	93.6	12000
6	2575	90.7	189400	94.1	11710
7	2590	89.3	190400	94.4	11350
8	2591	89.2	190400	94.4	11650
9	2584	88.9	190400	94.4	12110
10	2579	88.8	190100	94.2	12630
11	2566	88.3	189400	93.9	13100
12	2561	88.1	188700	93.5	13600
13	2564	88.2	189300	93.8	14120
14	2561	88.1	189200	93.8	14450
15	2504	86.2	186400	92.3	12700
16	2461	84.7	183800	91.1	14210
17	2418	83.2	181700	90.0	11970
18	2329	80.1	176000	87.2	13260
19	2293	78.9	174600	86.5	10100
20	2203	75.8	169100	83.8	11250

Table C.9: Monte Carlo response of a single counter to 3 GeV incident electrons.

for 1 and 3 GeV incident electrons. The photoelectron results for all of the blocks have ratios slightly greater than three between tables C.9 and C.8 since the shower maximum is closer to the PMT making the travel distance for the Čerenkov photons on the average shorter.

The resolution is better for 3 GeV incident electrons when compared to 1 GeV incident electrons. The resolution of energy deposited is between 0.05 and 0.07. For Čerenkov photons generated, the resolution is between 0.05 and 0.08. The photoelectron resolution is between 0.08 and 0.10.

Incident Energy (MeV)	% Energy Deposited	Generated Photons	Photo-Electrons
50	85.4	3163	181
84	84.7	5275	306
100	85.6	6336	367
200	85.7	12610	746
300	86.6	19140	1143
400	86.1	25390	1529
500	86.1	31470	1926
600	85.8	37910	2305
800	85.6	50840	3104
1000	85.8	63190	3900
1250	86.2	79510	4936
1500	86.4	95510	5977
1750	86.1	111100	6965
2000	86.2	127000	8007
2500	86.0	158200	10030
3000	86.1	190400	12120
3500	86.5	222600	14280
4000	86.2	253800	16260

Table C.10: The Monte Carlo response of shape 9 to different incident electron energies.

Shape 9 has been studied at many different energies. Table C.10 shows the result of 18 different incident energies for electrons. The photoelectron output can be characterized by

$$\text{Photoelectrons} = \text{Energy} \times (3.1795 + 0.10735 \times \ln \text{Energy}) \tag{C.1}$$

with Energy in MeV. The number of photoelectrons is not quite linear with respect to incident energy. The smaller incident energies have shower centers of gravity further away from the PMT, causing a greater absorption of photons of smaller wavelengths.

Block Shape Number	Pions Photo-electrons	Pions Ratio to 3GeV e^-	Cosmic Muons Photo-electrons	Cosmic Muons MeV Equivalent
1	1595	0.129	1478	366
2	1632	0.131	1526	375
3	1655	0.134	1557	389
4	1715	0.141	1613	408
5	1778	0.148	1685	436
6	1822	0.156	1733	459
7	1869	0.165	1814	494
8	1970	0.169	1881	501
9	2042	0.169	1952	501
10	2139	0.169	2046	500
11	2223	0.170	2082	490
12	2298	0.169	2197	494
13	2406	0.170	2291	498
14	2478	0.171	2325	495
15	2237	0.176	2041	492
16	2509	0.177	2193	467
17	2163	0.181	1858	479
18	2440	0.184	2028	466
19	1926	0.191	1520	461
20	2177	0.194	1684	459

Table C.11: The Monte Carlo response to punch through pions and cosmic ray muons.

C.3.2 Non-showering Particles

The non-showering particle photoelectron results all show a high tail to a gaussian distribution, see figure C.6. The results of 3 GeV incident pions and cosmic ray muons are presented in table C.11. The mean value of the distributions are in columns two and four. Column three is the ratio of photoelectrons for a 3 GeV incident pion to a 3 GeV incident electron. The ratio is dependent upon the length of the block since the number of Čerenkov photons generated is directly proportional to the path length of the pion. The ratios increase additionally when the electromagnetic shower of the incident electron is no longer able to be contained in the smaller blocks (greater shape number). The fifth column is the equivalent energy in MeV that a cosmic ray muon appears to have when using a 1 GeV incident electron as a reference response (assuming linear response to zero energy). The pattern of increase of the equivalent energy as the block number increases is the same as for the pions mentioned above.

The photoelectron resolution for the incident pion is between 0.10 and 0.12. Resolutions of 0.12 and 0.16 for most blocks, and increasing to 0.20 for the smaller blocks due to clipping, have been obtained for cosmic ray muon Monte Carlo results. Clipping is when a muon does not enter through the front face.

Pions and protons have been run at 2.5 and 4 GeV incident energies. At 4 GeV there is an increase in the photoelectron mean of 2% and 11% for pions and protons, respectively, compared to 2.5 GeV incident particles. This increase is caused mainly by the additional available energy for δ ray production. There is also an increase in β (a greater increase for the proton) which has a small effect upon the amount of Čerenkov light production.

For the smaller shapes, the effect of a pion entering a block at non-normal incidence has been investigated. A decrease of less than a percent of the photoelectron mean has been seen for an incident angle of one degree from the normal.

C.4 Comparison to Test Beam Studies

The two test beam studies that were undertaken to calibrate the central calorimeter and study the calorimeter response are discussed in section 4.2. Discussed here is how the Monte Carlo results compare to the studies performed.

C.4.1 AGS Tests Comparison

The Monte Carlo simulates the response of one counter. The Monte Carlo does not simulate the gains of the PMTs; it is assumed that the gain of the PMTs for every shape is the same and does not depend upon incident particle type. Comparison between Monte Carlo and the data is possible by taking ratio of results on a shape by shape basis. Column three of table C.11 is the ratio of photoelectrons from 3 GeV incident pions to electrons from the Monte Carlo. Making cuts on the incident position and direction from tracking available at the AGS, a similar ratio was calculated. Figure 4.6 shows the Monte Carlo photoelectron ratios and the AGS data ratios; the explanation of the ratio as a function of shape is given in section 4.2. The Monte Carlo is in good agreement with the data.

In section C.3.2, it is mentioned that there is a slight increase in photoelectron output (2%) for 4 GeV pions when compared to 2 GeV pions. The data collected at the AGS showed an increase of 7%. Simulations were done to see what effect the paper wrapping has upon the propagation of the Čerenkov photons to the PMT. Shape 11 has been investigated since such a counter was studied at the (AGS) with

BNL-AGS or Monte Carlo	Incident Beam Particle	Incident Energy (GeV)	Means Results Cloth	Means Results Paper	Means Cloth/Paper (%)
BNL-AGS	Electron	1	170	231	73.6
ADC	Electron	3	573	758	75.6
Measured	Pion	2	108	121	89.2
Means	Pion	4	116	133	87.2
Monte	Electron	1	3055	4251	71.9
Carlo	Electron	3	9312	13100	71.1
Photo-	Pion	2	2010	2223	90.4
electrons	Pion	4	2098	2361	88.9

Table C.12: Comparison of a shape 11 counter for white paper and dark cloth wrappings for Monte Carlo and AGS results.

and without paper wrapping. Table C.12 compares the measured ADC mean channel number and the Monte Carlo photoelectron results of studies of wrapping the counter in white paper or a dark cloth; there is good agreement.

Since part of the electromagnetic shower escapes the incident block, a study of sharing of energy was done on the data taken at the AGS. The eight modules' outputs that surround the hit counter were summed with the hit counter's output for a total charge collected. A Monte Carlo of nine modules with the correct block geometry would be complicated using the EGS4 code. A correction of the photoelectron results for incident electrons was made by multiplying by the ratio of Čerenkov photons generated within the large block to those within the shape. This assumes that the percentage of Čerenkov photons resulting in photoelectrons is the same for photons generated within the shape as for the photons generated outside of the shape and within the large block (i.e. the surrounding eight modules). Figure 4.7 shows the adjusted Monte Carlo results and the summed nine counter responses ratios.

Data or Monte Carlo	Shape Number	Electron Energy of 84 MeV	Electron Energy of 1 GeV	84 MeV to 1 GeV Ratio
NPL and	01	22.3	303	0.0736
BNL-AGS	09	21.6	271	0.0797
ADC	15	22.3	267	0.0835
Measured	17	24.7	265	0.0932
Means	19	17.3	232	0.0746
Monte	01	307	4043	0.0759
Carlo	09	306	3900	0.0785
Photo-	15	332	4150	0.0800
electron	17	307	3881	0.0791
Results	19	260	3299	0.0788

Table C.13: Comparision of 84 MeV and 1 GeV electron responses from the Monte Carlo and UINPL data.

C.4.2 UINPL Tests Comparison

A common light source used at both the AGS and UINPL was a bismuth source encased in scintillator plastic glued to the front face of each block. The response to incident electrons has been compared to the response to the bismuth source. The ratio of the responses to the incident 84 MeV electrons at the UINPL and 1 GeV electrons at the AGS was determined. Monte Carlo simulations of 84 MeV incident electrons have been run for the shapes that were tested at the UINPL. Table C.13 shows the ratios for the five counters. The ratio of responses to incident electrons of 84 MeV and 1 GeV is shown in the last column of table C.13 for the Monte Carlo and the two test beam studies. The Monte Carlo agrees with the data from the larger counters in which the incident electron position and electromagnetic shower size are not factors. A paper test done to one counter at the UINPL shows a decrease without the paper of 72.3% which is comparable to results shown in table C.12.

C.5 Discussion

The Monte Carlo that was developed has been useful in predicting the response of a single central calorimeter counter to different incident particles. The results of the Monte Carlo were used successfully in the initial calibration of the counters (section 4.1). Test beam results have been compared to the Monte Carlo results. The comparisons show that, for different incident particles and/or different wrappings of the counters, the Monte Carlo can accurately predict responses.